THE OVERVIEW OF NEW CARBON PROPELLER DEVELOPMENT FOR 32KG GROSS WEIGHT AGRICULTURAL MULTICOPTER (OCTOCOPTER)

Deog-Kwan Kim, Seong-Yong Wie, Jaerim Song, Hee Jung Kang, Taejoo Kim and Youngjung Kee
(Rotorcraft Research Team, Korea Aerospace Research Institute, KARI)

Abstract

This paper describes the general overview of new carbon propeller development for 32kg Gross Weight agricultural multicopter (Octocopter drone). Based on the design process of helicopter rotor blade, KARI conducted the carbon propeller development. All tools and facilities related to develop helicopter rotor blade were applied in this program. This paper shows the main research activities such as aerodynamic design and analysis, structural design and analysis, fabrication and investigation, ground and flight test. Finally the flight time of the multicopter using the improved carbon propeller has increased compared to existing beachwood propellers by more than 20% through improved aerodynamic performance and reduced carbon propeller weight. This results was campaigned in 2015 Creative Korea-Exposition. Through this research, KARI had a good opportunity in drone industry to localize carbon propeller and improve drone performance.

1. INTRODUCTION

1.1. Background

Drone (UAV) was introduced to public people world widely in CES 2015. Especially the quadcopter which is one type of multicopters was very popular in people who enjoy personal hobby and leisure. From this worldwide trend, domestic company had started to pay attention to drone (UAV) market. Specially, the drone for agricultural and industrial purpose gave an impressive attention to government officers, industrial people and agricultural farmers. From this trend, one of companies which operated agricultural multicopters had a plan to improve its own vehicles. This company requested KARI to improve its existing representative multicopter since KARI had experienced in rotor blade development for over 20 years. The company's multicopter (named as AFOX-1A) had 8 wooden propellers (beachwood). So, the locally fabricated and improved propeller was required to get vehicle's efficiency. KARI decided to improve propeller primarily in viewpoint of new propeller's aerodynamic design and structural design with light material after investigation of several items. For this short term program, KARI had setup the development process of high performance carbon propeller to finish earlier based on helicopter rotor blade's experience. [1]

1.2. Program Overview

This program was launched on the 1st of March in 2015 and ended on the 30th of November in 2015 (9 months). This program was funded by KARI internal budget. The final goal of this program is to develop new high performance carbon propeller for 32kg gross weight agricultural octocopter, to transfer technologies to company and to demonstrate in 2015 Creative Korea-Expo finally. The program goals such as 5% figure of merits improvement and more payload were setup. Figure 1 shows some of representative multicopters.

At the 1st stage, ClarkY airfoil were surveyed as a primary candidate airfoil within limited time. Based on this airfoil, the thickness and curvature were fitted after considering trailing edge minimum thickness, root thickness and so on. To analyze airfoil, XFOIL was used. It is viscous-panel method since this tool was effective in low Reynolds's environment including transient model. Propeller's planform design was conducted to minimize induced drag through optimize twist angle and chord length variation. To analyze this prediction, QPROP tool was used which was worked based on Blade Element/Vortex method. For precise performance analysis, the CAMRADⅡ was used. After comparison of each new designed propeller, the final propeller was selected. KARI in-house code (KSec2D) which is for blade sectional analysis code was used to do sectional design of this propeller. From this sectional design, the propeller's sectional properties were calculated. Finally, this propeller was fabricated. After checking the sectional properties and weight, the ground rotational test of new fabricated carbon propeller was conducted.

At the 2nd stage, ground propeller rotational test was conducted. The both of existing and new developed propellers were conducted and measured the thrust and torque to get figure of merit. After verification of this ground test, the flight test was conducted in the company's flight test site. The performance improvement was verified from this flight test finally. [2-3]. Figure 2 shows original octocopter and KARI's developed new propeller-installed octocopter in this development program.

Figure 1: the several types of multicopters

Figure 2: Original Octocopter vs Improved Octocopter

2. MAIN RESEARCH ACTIVITIES

This sections describes main research activities related to develop new carbon propeller. First, aerodynamic design and analysis was described. Second, propeller design and performance analysis were described in detail. Structural design and analysis was described. And dynamic and load analysis was shown. Fabrication and Qualification of carbon propellers were described. Finally ground and flight test were described

2.1. Aerodynamic Design & Analysis

For the selection of the airfoil, the flow conditions applied to the propeller blades should be checked After confirming Reynolds number corresponding to the rotational speed, the airfoil is selected and airfoil aerodynamic data base (lift and drag coefficients) is calculated using XFOIL(viscous-panel method). Since the rotational speed is less than Mach No. 0.4, the incompressible airfoil solver XFOIL is suitable for use.

In order to compare the performance of the designed propeller, the shape of the baseline propeller was confirmed by 3D scanning. The aerodynamic force DB of baseline propeller airfoil is calculated under the same flow conditions of design propeller airfoil.

Modified Clark-Y airfoil was selected for the airfoil considering the Reynolds number range and the operating rotational speed. The selected airfoil is an airfoil modified from the Clark-Y airfoil [1] considering its composition and performance, and it considers the trailing edge thickness including the actual manufacturing error.

2.2. Propeller Design and Performance Analysis

The propeller planform design was implemented by QMIL/QPROP program developed by Mark Drelar of MIT University [4]. The QMIL/QPROP program generate the propeller chord length and twist angle distribution along the span to minimize the induced power for given propeller radius, number of blades, rotational speed, sectional lift coefficient of airfoil and the required thrust condition.

The propeller root location and maximum cord length were set to 10% and 30% of the propeller radius and the root thickness of the airfoil was increased to ensure the structural safety margin. The distribution of chord length and twist angle in the root region of the propeller were modified from the result of QMIL/QPROP. Figure 3 shows the distribution of cord length and twist angle along the span of the propeller.

Figure 4 shows aerodynamic performance of the designed propeller compared to the propeller applied to the original multicopter (AFOX1A). The analysis was conducted by using CAMRAD-II, which is comprehensive aeromechanics analysis program [5]. Thrust of the designed propeller is much higher than the propeller of AFOX1A on full range of rotational speed. The required power also reduced than that at the same thrust condition. Finally, figure of merit, aerodynamic performance efficiency, of the designed propeller is increased about 0.1 ~ 0.2 than the propeller of AFOX1A on full range of thrust. On the operating condition, which is the condition of about 40 N of required thrust, the required power reduced about 16% and figure of merit is increased about 0.15.

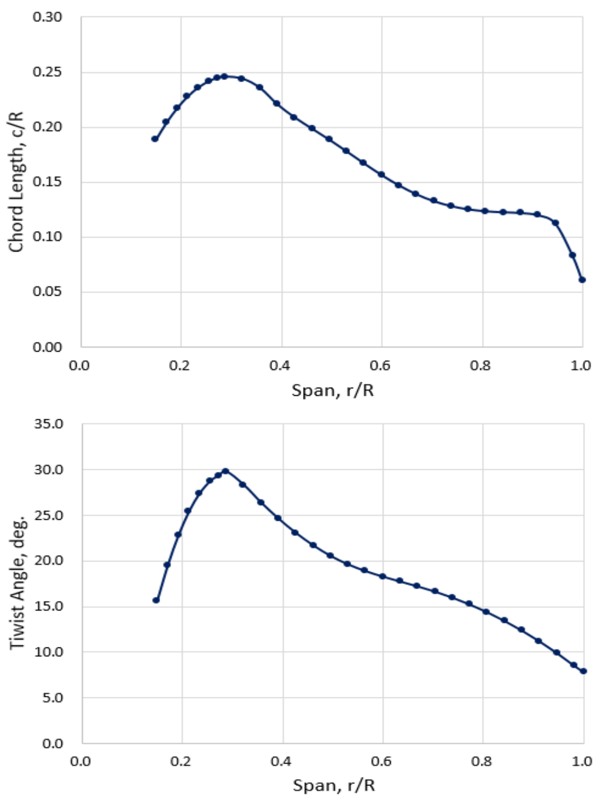

Figure 3 The Chord Length and Twist Angle Distribution of the Designed Propeller

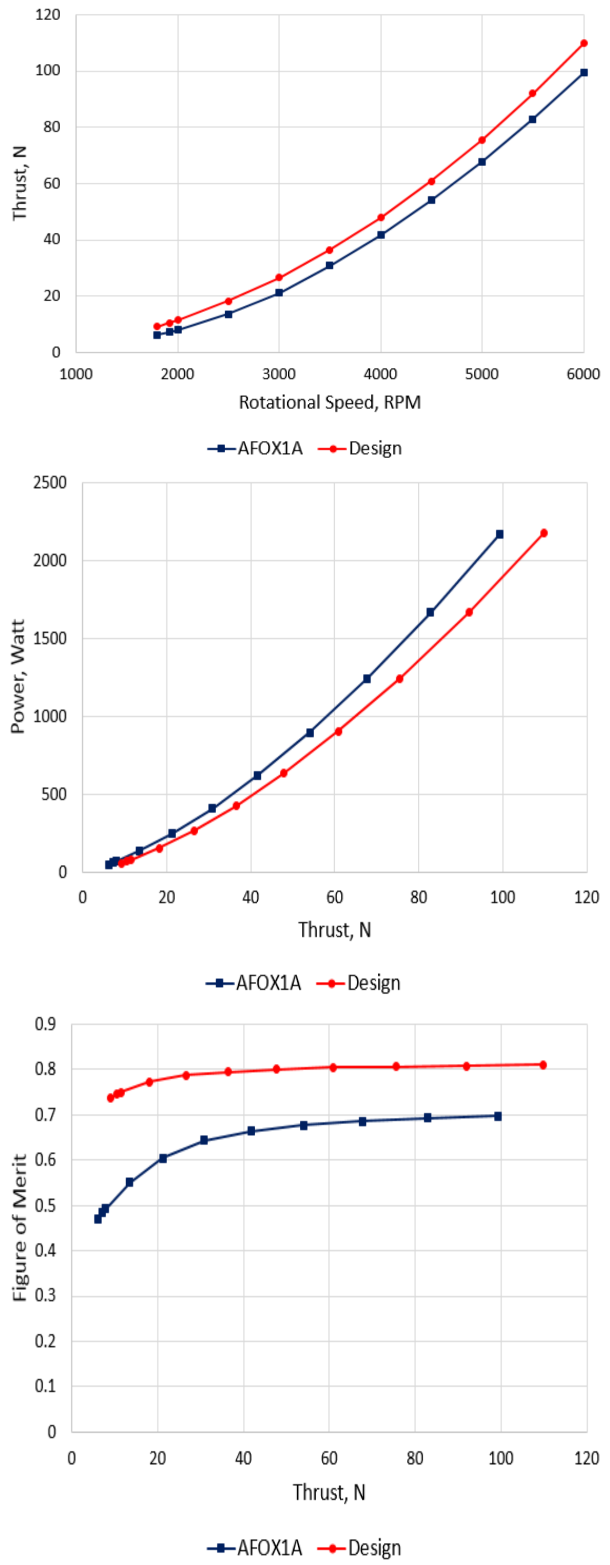

Figure 4 Comparison of Propeller Performance between the AFOX1A and the Designed Propeller

2.3. Structural Design & Analysis

2.3.1 Requirement Criteria Selection for Section Design

For the section design of the propeller, the criteria for strength and stiffness must be determined. Since the propeller used in the multi-copter has a short length, elastic deformation more than the second is hardly generated during operation, so it can be assumed as a rigid beam model. Therefore, if the stiffness value of the propeller is greater than the stiffness value of the existing shape propeller, it can be judged that there is no significant influence on the propeller operation including the possibility of resonance. Also, when the section stiffness is high and the material strength is high, it is judged that there is no structural problem within the same load operating range. In order to select the stiffness criterion for the sectional design of the improved propeller, the cross section analysis of the existing propeller was performed.

The cross section analysis position was selected by increasing the propeller center direction from the 5% position to the 95% position in 10% increments in the direction of the propeller end (Figure 5). Propeller shape information was acquired through the 3D scan of the propeller, and the two - dimensional cross - sectional shape for each position was extracted using this information. The section analysis was performed using KSec2D, [6] a two-dimensional finite element section analysis program, and the propeller material properties were extracted from the wood handbook. [7]

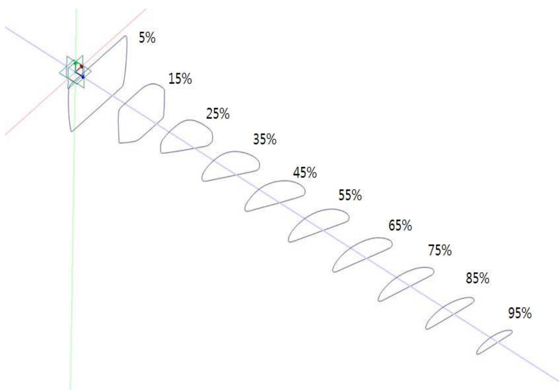

Figure 5 Propeller Analysis Section

2.3.2 New Carbon Propeller Section Design and Analysis

For the section design of the propeller, orthogonal carbon fiber (Carbon Fabric) and unidirectional carbon fiber (Carbon UD) were used. Considering the centrifugal force and lift level generated during propeller operation, we did not apply tension / bending direction reinforcement structures such as spar or honeycomb core, and simplified the internal shape. The inner shape was formed by hard foam and the composite carbon fiber was laminated on the outside to construct the skin. However, Beech wood was used for the inner structure from the center of the hub to the span direction to 10%, considering bolt hole for fastening. The composite laminate pattern is shown in Figure 6 and Table 1

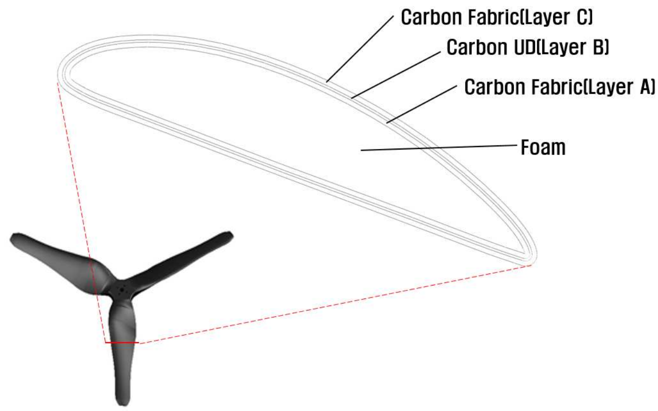

Figure 6: New Carbon Propeller Section Shape

Proposed Stacking Pattern	CF[(±45)]CU[(0)$_2$]CF[(±45)]

Table 1: Composite Material Stacking Pattern for New Carbon Propeller

Sectional analysis of each laminated pattern was performed on new carbon propeller shapes. The analytical sections were divided into 10% to 10% positions in the span direction based on the propeller hub center. The material properties used in the section analysis of the propeller are shown in Table 2. [8] The following figures 7 and 8 show the results of the new carbon propeller cross section analysis and the results of the existing propeller cross section analysis for the tensile / bending / twisting stiffness values and mass per unit length. The weight of the new carbon propeller predicted by the section analysis is 80.6g.

Material	Properties	
Carbon UD	E_{11}(N/mm^2)	1E+05
	E_{22}(N/mm^2)	7E+03
	G (N/mm^2)	3E+03
	ρ(N/mm^3)	2E-06
Carbon Fabric ±45	E_{11}(N/mm^2)	1E+04
	E_{22} (N/mm^2)	1E+04
	G (N/mm^2)	3E+04
	ρ (N/mm^3)	2E-06
Foam	E_{11}(N/mm^2)	9E+01
	E_{22} (N/mm^2)	9E+01
	G (N/mm^2)	2E+00
	ρ (N/mm^3)	5E-08

Table 2: Material Properties used in Section Analysis of New Carbon Propeller

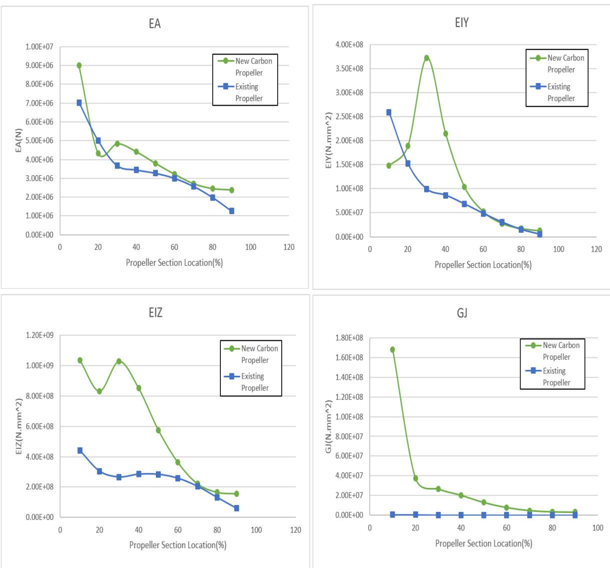

Figure 7: Sectional Analysis Results of New Carbon and Existing Propeller – EA/EIY/EIZ/GJ

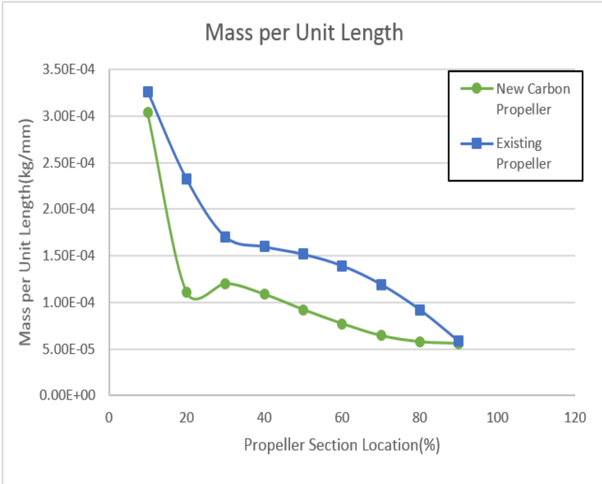

Figure 8: Sectional Analysis Results of New Carbon and Existing Propeller – Mass per Unit Length

2.4. Dynamic & Load Analysis

2.4.1 Dynamic Analysis

For the propeller model with cross-sectional design, non-rotational and rotational natural frequency and mode shapes of the propeller were analyzed using the finite element analysis program Midas-NFX. In order to take into consideration the internal structural characteristics of the propeller, a skin was discretized by a 2-dimensional shell element (4-node, CQUAD4), and a foam core was discretized by a 3-dimensional solid element (8-node, CHEXA8). In addition, a clamped geometric boundary condition was added based on the bolt-hole at the center of the propeller to reflect the condition that the propeller is fixed to the electric motor, and the finite element analysis model used in the present study is shown in Figure 9. In order to analyze the change of the natural frequency according to the rotation speed of the propeller, the modal analysis was performed while increasing the rotation speed of the propeller up to 6,000 rpm. As shown in Table 3, as the rotational speed of the propeller increases, it is confirmed that the natural frequencies of all the modes are increased by the influence of the centrifugal force. Also, at 6,000 rpm, the natural frequencies of the fundamental flap, lag and torsion modes were confirmed at 630 Hz, 1,352 Hz, and 2,116 Hz. Furthermore, it is confirmed that the dynamic instability due to the resonance does not occur because it is sufficiently separated from the natural frequency of the airframe.

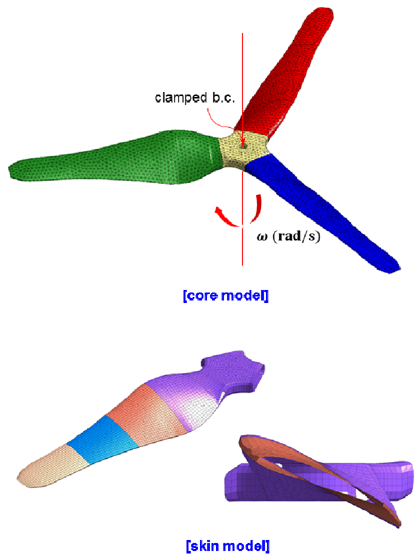

Figure 9: Midas-NFX analysis model

RPM	1st flap	2nd flap	1st lag	1st torsion
0	617	1,966	1,354	2,098
1,000	617	1,966	1,354	2,099
2,000	618	1,966	1,354	2,100
3,000	620	1,966	1,355	2,102
4,000	622	1,967	1,352	2,104
5,000	625	1,967	1,357	2,106
6,000	630	1,968	1,352	2,116

Table 3: Natural frequencies w.r.t the propeller rotating speed

2.4.2 Load & Structural Analysis

CAMRAD II, a comprehensive helicopter analysis program, was used to investigate the centrifugal force and bending moment distribution on the cross section according to the operating conditions of the propeller. As shown in Figure.10, the propeller analysis model consists of 23 aerodynamic panels in the radial direction to calculate the aerodynamic force according to the propeller rotating speed and angle of attack, and 8 structural elements were applied to account for elastic deformation. Figure. 11 shows the bending load distribution, and the flap and lag bending moments shows a highest value at the 25%R section, and the centrifugal force by the propeller rotation was the largest at the root. As shown in Figure 12, the structural margin of the carbon fiber used for the skin was found to be at least 1.7 and structurally safe.

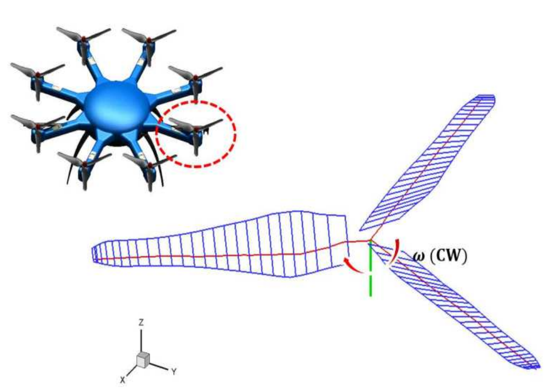

Figure 10: CAMRADII analysis model

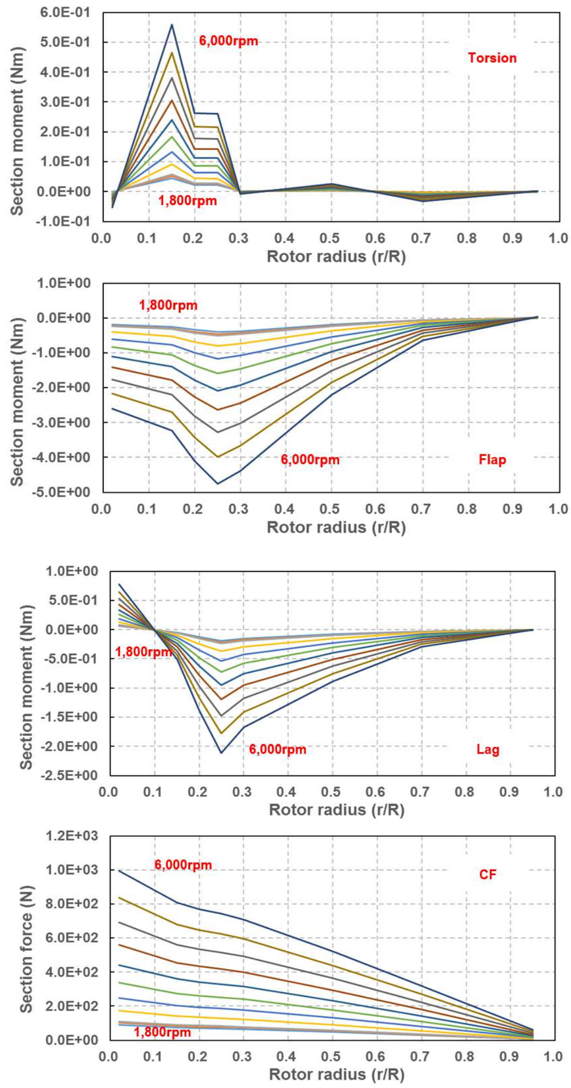

Figure 11: Bending moments and CF force distributions

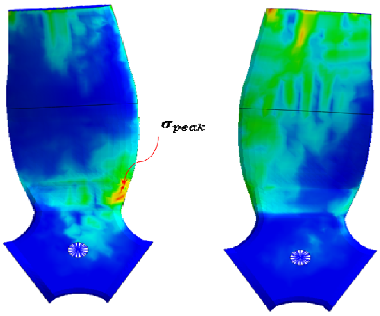

Figure 12: Finite element analysis results (peak stress)

2.5. Fabrication

Propeller fabrication was carried out by applying the proposed composite laminate shape through the section design. The hot press method was used as a propeller manufacturing method considering that the lamination pattern and the inner shape are simple. In order to construct the internal shape, a hard foam was processed, a composite material was laminated on a hot press mold, and high temperature / high pressure was applied to produce a composite material propeller. Figure 13 shows the propeller mold and propeller construction.

Figure 13: New Carbon Propeller Production Shape and Mold

2.5.1 Qualification Check

The shape of the propeller was qualified. The qualification items were classified into external dimensions and static balancing. A template was used to verify the external dimensions. To qualifying external dimension, chord length at 100, 150, and 200 mm span positions from the propeller center and total span length were measured.(Figure 14) For static balancing, propeller balancing tools was used.(Figure 15) In addition, the weight of the propeller was measured and compared with the predicted weight. The average of the measured weights was 82.75 g, which showed an error of about 2.58% compared with the predicted weight.

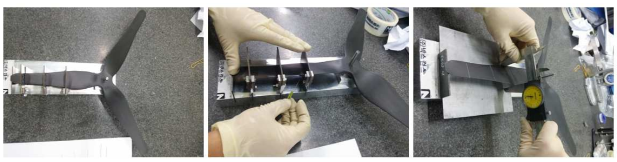

Figure 14. New Carbon Propeller Qualification Check – External Dimension

Figure 15. New Carbon Propeller Qualification Check – Static Balancing

2.6. Ground and Flight Test

2.6.1 Ground Test

LabVIEW and DAQ devices of National Instruments (NI) were used to control the BLDC motor and collect test data such as thrust, power(torque) and rotating speed from load cell, torque meter and photo sensor. Figure 16 shows the diagram of test devices

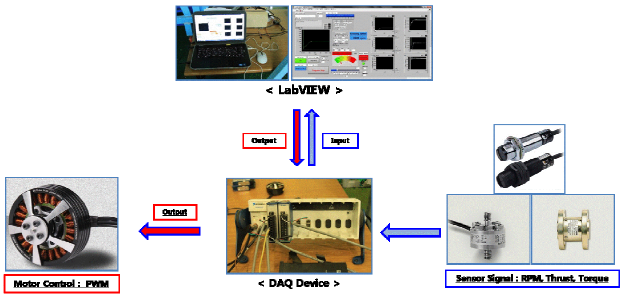

Figure 16 Diagram of Test Devices

The following program for test in figure 17, based on LabVIEW, made for generating PWM (Pulse Width Modulation) signal, and sends it through NI DAQ to electrical speed controller (ESC) to control the rotating speed of the BLDC motor. This program also has a function to collect and save the measured aerodynamic performance (thrust, power) and rotating speed of motor as a text file.

The following figure 18 shows the test devices that were used the ground performance test of the designed and baseline propeller. The performance test was performed by measuring the propeller from 1000 rpm to 4600 rpm at 200 rpm intervals and comparing the results.

It can be seen in figure 19 that the hover flight efficiency (Figure of Merit) of the designed propeller is improved compared to the baseline propeller in the whole revolution speed range and the performance improvement is about 7 ~ 8% in the range of 3000 ~ 4500rpm, which is the operation area of AFOX1A. At 2800 ~ 3200rpm, the vibration increases so that the trend of the test results is different from the other speed ranges.

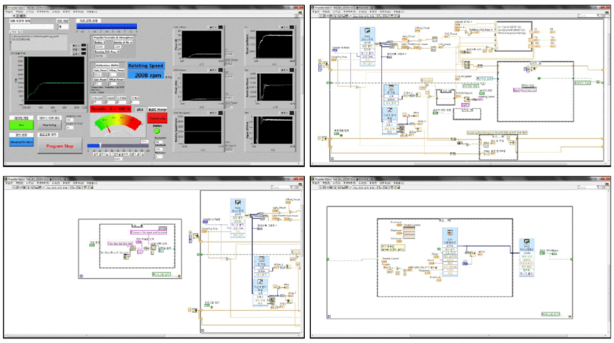

Figure 3 Program for Ground Performance Test

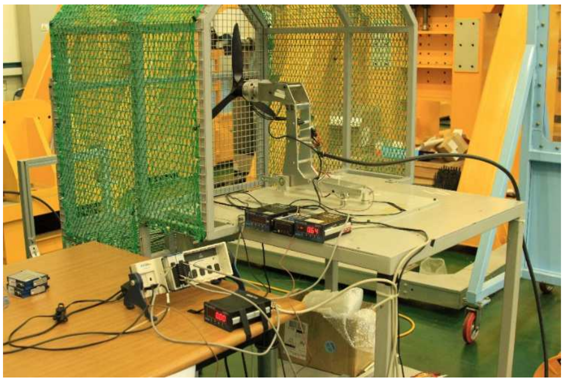

Figure 18 Ground Rotational Test Rig of Propeller in KARI

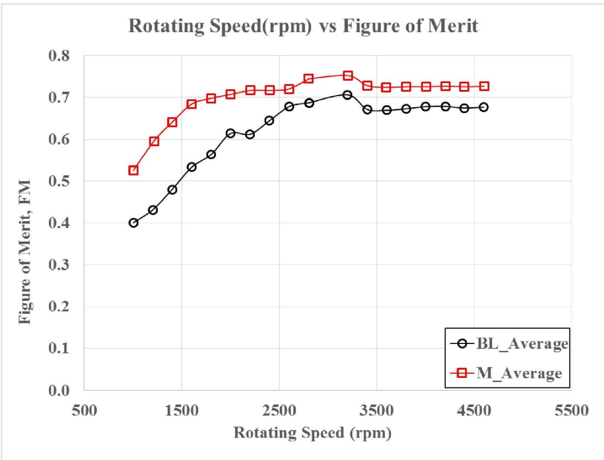

Figure 4 Comparison of Figure of Merit

2.6.2 Flight Test

Flight tests were performed to compare flight time of baseline (AFOX1A) and designed propellers. The dark blue multi-copter is equipped with a designed propeller, and the red multi-copter is equipped with a baseline propeller as AFOX1A. Figure shows the Flight Test of Designed and AFOX1A Propeller.

Figure 5 Flight Test of Designed and AFOX1A Propeller

The flight test was carried out by measuring flight time with payloads of 0, 10 and 15 kg. In the case of the new body frame, it was tested in a reduced weight compared to the baseline body by reducing the weight according to the propeller design and improving the weight of the gas itself. Therefore, the test results are compared assuming that the same weight is used when comparing flight time. Table 4 and 5 shows the flight test results with Take-0ff Weight and Empty Weight Condition.

Payload (kg)	Take-Off Weight(kg)	Empty Weight(kg)
0	17.6	17.6
10	27.6	17.6
10 (with skin)	31.2	21.234
15	32.95	17.95

Table 4 Weight and Flight Time of Baseline Propeller and Body Frame

Payload (kg)	Take-Off Weight(kg)	Empty Weight(kg)
0	16.4	16.4
10	26.4	16.4
12 (with skin)	31.847	19.847
15	31.75	16.75

Table 5 Weight and Flight Time of Designed Propeller and Body Frame

2.6.3 Campaign

Tests for flight time comparison were performed as shown in figure 21, with the payload (weights) shown in Tables 4 and 5.

Figure 6 Flight Test for Measuring Flight Time.

Baseline		Designed	
Take-Off Weight(kg)	Flight Time(min)	Take-Off Weight(kg)	Flight Time(min)
17.6	14.5	16.4	18.8
27.6	4.1	26.4	6.15
31.2	1.88	31.847	2.58
32.95	1.67	31.75	3.15

Table 6 Results of Flight Test

Based on Table 6, assuming that the empty weight and the take-off weight are 21kg and 32kg, respectively, aerodynamic performance improvement of the new multicopter equipped with the designed propeller is 35% in the empty weight and 83% in the takeoff weight.

2.7. Result

Performance analysis using CAMRADII was performed to compare the performance of the design profile with the baseline propeller. We also confirmed the final performance of the propeller designed through the rotation test.

2.7.1 Test Result

In the case of the figure of merit for the propeller, it can be confirmed that the design shape is improved compared with the baseline shape.

Also, the amount of current consumed by the design shape is also reduced compared to the baseline shape. In the ground test, it is shown that the design propeller is aerodynamically more efficient.

In the flight test, multi-copter with design propeller flew longer than multi-copter with baseline propeller. From the figure below, it can be seen that the flight time decreases as the gross weight increases, and the overall flight time of the improved shape propeller is greater than baseline propeller.

The flight time of the multi-copter using the improved propeller has increased by more than 20% through improved aerodynamic performance and reduced propeller weight. Figure 15 shows the improvement of figure of merit. Figure 16 shows the electric current comparison. Figure 17 shows the flight time comparison.

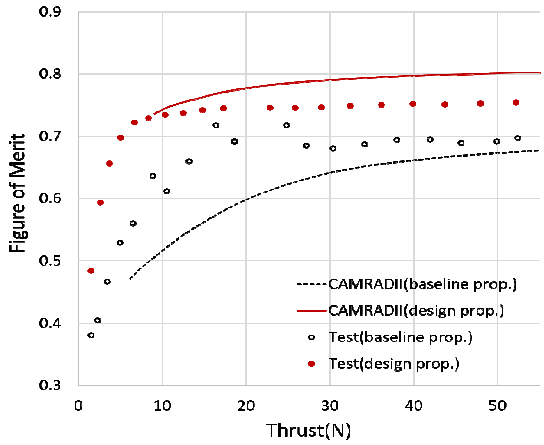

Figure 15. Figure of Merit

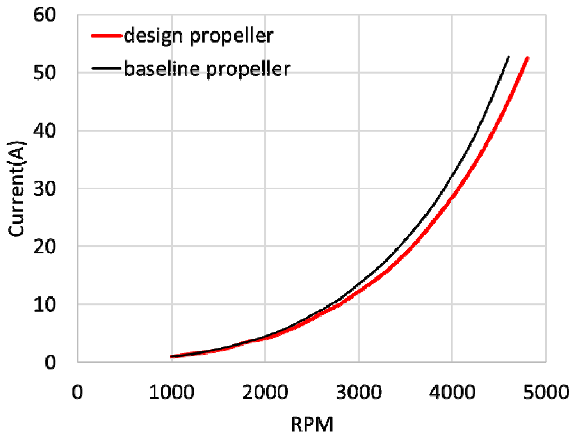

Figure 16. Current comparison

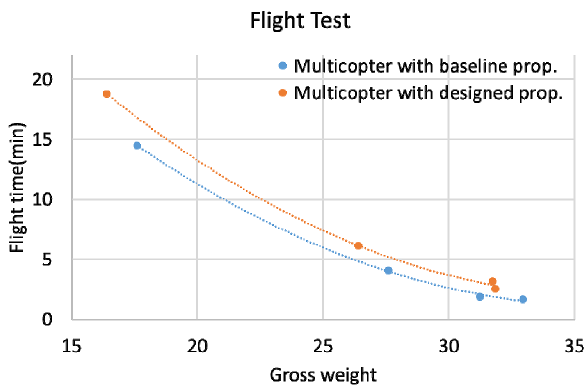

Figure 17. Flight time of Multicopter

3. CONCLUSION

This paper describes the general overview of new carbon propeller development for 32kg Gross Weight agricultural multicopter (Octocopter drone). Based on the design process of helicopter rotor blade, KARI conducted the carbon propeller development. All tools and facilities related to develop helicopter rotor blade were applied in this program. This paper shows the main research activities such as aerodynamic design and analysis, structural design and analysis, fabrication and investigation, ground and flight test. Finally the flight time of the multicopter using the improved carbon propeller has increased compared to existing beachwood propellers by more than 20% through improved aerodynamic performance and reduced carbon propeller weight. This results was campaigned in 2015 Creative Korea-Exposition. Through this research, KARI had a good opportunity in drone industry to localize carbon propeller and improve drone performance.

4. REFERENCES

[1] http://m-selig.ae.illinois.edu/ads/coord_database.html

[2] http://www.crn.com/slide-shows/channel-programs/300075327/the-top-25-products-from-ces-2015.htm/pgno/0/19

[3] J. Gordon Leishman, "Principles of Helicopter Aerodynamics", University of Maryland, Cambridge University Press 2006

[4] Drela, M., QProp Propeller/Windmill Analysis and Design, Ver. 1.22, Massachusetts Institute of Technology, Cambridge, MA, http://web.mit.edu/drela/Public/web/qprop, 2011

[5] Johnson, W., CAMRAD II, Comprehensive Analytical Model of Rotorcraft Aerodynamics and Dynamics, Release 4.9, 2012

[6] Park, I. J., Jung, S. N., Cho, J. Y., and Kim, D. H., "A Study on Calculation of Cross-Section Properties for Composite Rotor Blades Using Finite Element Method," Journal of the Korean Society for Aeronautical and Space Sciences, Vol. 37, No. 5, 2009, pp. 442~449.

[7] Kretschmann, D. E., Wood Handbook: wood as an engineering material, Centennial Edition, United States Department of Agriculture Forest Service, Madison, 2010, Chapter 5

[8] Park, S. O., Lee, M. H., Woo, D. H., and Shin, J. W., "Composite Material Allowables for Development of EAV", KARI Report, 2014.